

The supramolecular physics of the ambient water

Alexander Kholmanskiy

Science Center «Bemcom», Moscow, Russia

allexhol@ya.ru, <http://orcid.org/0000-0001-8738-0189>

Abstract

The anomalous properties of ambient water at normal pressure and temperatures from 0 °C to ~ 100 °C are mainly due to the physics of hydrogen bonds in supramolecular structures (SMS). The lifetime, composition, and degree of ordering of SMS are temperature dependent and this affects the temperature dependences (TDs) of all water characteristics. To clarify the nature of the movements responsible for SMS restructuring, we used the activation energies (E_A) of the known TDs 13 characteristics of water and 10 parameters of its microstructure. The bimodality of thermodynamics of water was taken into account, dividing E_A into two components - thermal (E_T) and conformational (E_R). The values of E_A , E_R and E_T were determined using Arrhenius approximations, and the thermal component TDs was represented by the function T^β . A physically adequate choice of β values ensured the accuracy of the approximations. It was found that E_A for dynamic characteristics is comparable to the hydrogen bond energy and an order of magnitude greater than E_T . For the static characteristics of water $E_R = E_T$ at extreme points. The values of E_A macro characteristics and the corresponding parameters of the microstructure of water are qualitatively correlated with each other. Based on these data, the extremums TDs of density and isobaric heat capacity, as well as the kinks of dynamic characteristics TDs at 25 °C, were associated with the transformation and decay of ice-like hexagonal clusters in SMS. The extremums TDs of compressibility and sound velocity were explained by the reaction of the molecular dynamics of water to the action of an anisotropic external factor. Excessive external pressure similarly affected the characteristics of water. Spontaneous polarization of Drude oscillators at extreme points of TDs static characteristics was used as the basis for the long-range mechanism in SMS phase transitions. For the role of the order parameter that triggers this process, the frequency of oscillations of the O-H bond was proposed.

Keywords: water; abnormal; bimodal thermodynamics; Arrhenius approximations; polarization.

Introduction

Thanks to water on Earth a hierarchy of living systems arose and developed with homo sapiens at the head [1-3]. Therefore, anomalies in the properties of liquid water under normal conditions can be attributed to the manifestation of the Anthropic Principle at the molecular level [4]. First of all, we are talking about the features of temperature dependences (TDs) of the properties of liquid water at atmospheric pressure and temperature (T) from 0 °C to 100 °C. Under these conditions TDs density (ρ), molar volume (v), isobaric heat capacity (C_P), thermal conductivity coefficient (κ), isothermal compressibility (γ), sound velocity (V), dynamic viscosity (η), dielectric constant (ϵ), self-diffusion coefficient (D), refractive index (n_D), chemical shift (δ), spin times (T_1) and dielectric relaxation times (τ_D) are unusual and some of them have extrema or kinks [5-9]. Despite numerous experimental and theoretical studies of the structure and dynamics of liquid water, the molecular mechanism of the occurrence and differentiation of TDs anomalies of water characteristics is still unknown [8, 11, 12].

The structural dominant of the three-dimensional molecular structure of water is the near tetrahedral geometry of the electronic orbitals of the oxygen atom in the free H₂O molecule [6]. This geometry is minimized in energy by the formation of four tetrahedral hydrogen bonds (HBs) and their configuration reaches the utmost stability in the structure of ice-like hexagonal clusters (W_6) at $t = 0$ °C [8, 13]. The absorption band of W_6 lies in the region of 200-250 cm⁻¹ (Fig. 1b). The nature of molecular motions and bonds in liquid water is reconstructed from specific changes in the spectral parameters of liquid water and the radial distribution functions $g_{OO}(r)$, $g_{OH}(r)$, $g_{HH}(r)$ (Fig. 1a). For this, stationary and pulsed methods of IR, Raman, X-ray and neutron spectroscopy are used together with computer simulation of molecular dynamics [10-22]. To explain the anomalies in the static characteristics of water at ambient conditions (ρ , v , C_P , γ), the hypothesizes the existence of two metastable liquid phases – high density liquid (HDL) and low density liquid (LDL) [10-21]. Using the methods of X-ray spectroscopy and x-ray Raman scattering, it was established [11, 22] that up to 25 °C in the first coordination shell of LDL water prevail structure with the four tetrahedral HBs characteristic for hexagonal ice (Ih) [13]. Upon heating from 25 °C to 90 °C, 5 to 10% of these bonds are converted to two hydrogen-bonded configurations with one strong donor and one strong acceptor HB and LDL water goes into HDL water. The experiment

estimates the fraction of the tetrahedral configuration of LDL water at ambient conditions to be 20–40%, however, from molecular dynamics simulations it follows 60–80% [10, 17, 22].

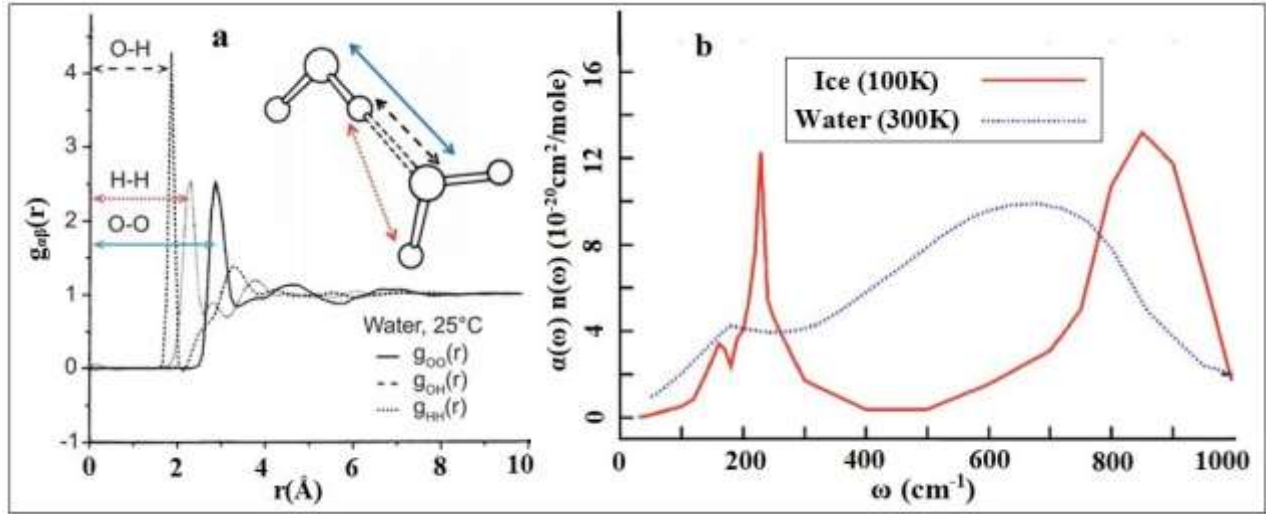


Fig. 1. (a) Partial pair distribution functions obtained from neutron diffraction, from [16]. (b) Experimental far-IR absorption spectra of ice and liquid water. Figure from [14].

In works [5, 8–10, 13, 23–28] suggest that the molecular mechanism of water anomalies is based on the physics of dynamic supramolecular structures (SMS) corresponding to “instantaneous” configurations of HBs network structures and correlated molecular motions. In SMS, the number of HBs, their energy, and their lifetime vary widely. These variations of HBs affect intermolecular interactions and the dynamics of SMS, which are based on inhibited rotational and translational movements of molecules. The range of their energies is limited above the energies of the HB (E_H) [5]. SMS rearrangement reactions with an activation energy (E_A) lower than E_H dominate in TDs anomalies of static (ρ , v , C_P) and conditionally static (κ , γ , V , ε) water characteristics [8, 24]. The dynamic characteristics (η , D , τ_D , T_I) have E_A values of the same order as E_H . In the thermostationary state at constant T , water is a reservoir of energy IR quanta, the action of which is manifested by Brownian motion, and the energy spectrum corresponds to the blackbody radiation band. The wavelength at the maximum of this band is determined by the Wien displacement law: λ_{\max} (m) = 0.0029/ T [24]. This band for $T > 240$ K will overlap with the IR absorption spectrum of water in the region of wave numbers (ω) less than 1000 cm^{-1} (Fig. 1b).

The structure of liquid water at $273 < T < 373$ K consists of free and encapsulated molecules, hexagonal clusters (mainly W_6), various voids, linear chains, and three-dimensional networks of HBs (Fig. 2). Extreme points TDs of water properties can be considered critical points [30] of

phase transitions between different SMS conformations. To describe the physics of these transitions, the formalism of the nonequilibrium thermodynamics of phase transitions in clusters is suitable, in which configurational excitation is represented through the transformation and diffusion of voids in a cluster structure [31]. The concept of voids distinguishes configurational degrees of freedom from the oscillatory ones described by the equilibrium Boltzmann statistics. The energy of equilibrium thermal motions of molecules selectively activates the reactions of SMS rearrangements and this corresponds to the activation character of diffusion and transformation of voids [31]. Within the framework of this formalism, the element of void and vacancy in SMS [9, 31] can be considered a thermodynamic variable that characterizes the motion and energy of bonds of the molecules forming the element of void.

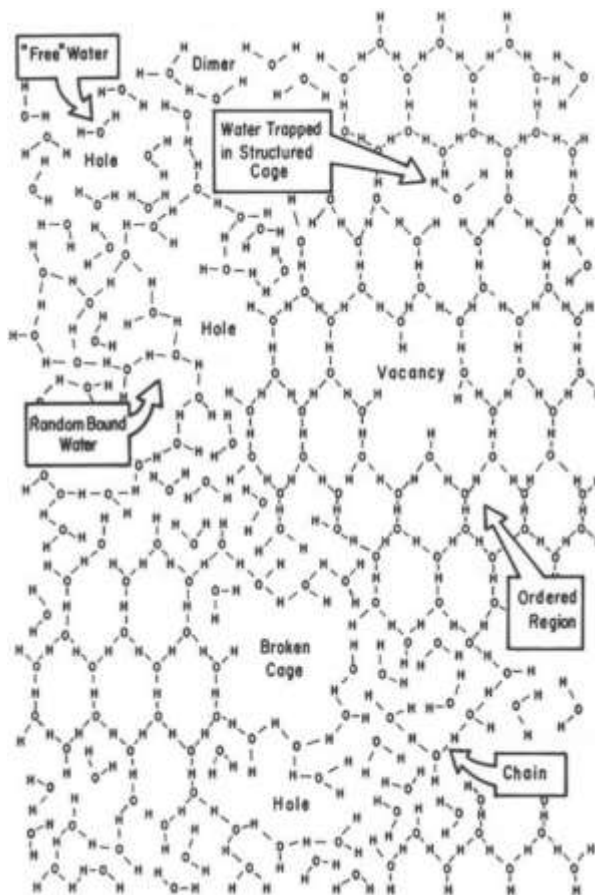


Fig. 2. The liquid water-structure complexity is reproduced in a two-dimensional plot for the sake of visualizing some of its characteristics [29].

Water inherits the void structure during the melting of hexagonal ice Ih and W_6 dominates the structure of the elements of the void up to 25 °C [5, 6, 8, 9, 22, 24, 32]. The division of void statistics into Boltzmann (vibrational) and configurational ones corresponds to two types of

thermodynamics of water, which attracted its dynamic and static characteristics for analysis of TDs [8, 24]. I-type thermodynamics describes the reactions of the breakdown of HB and the release of a water molecule from a cell. II-Type thermodynamics are based on transformation reactions of HBs network configurations. The parameters of the water structure and its rotational-vibrational spectra depend on T. From the Arrhenius f_A -approximations of these TDs, one can find the order of magnitude of the E_A rearrangements of the SMS and the probable nature of molecular motions.

In the metastable state of supercooled water at $T < 273$ K, both statistics and the corresponding types of thermodynamics will become inadequate due to inhibition of the self-diffusion process, freezing of conformational degrees of freedom, and an increasing role of impurities and gases in the initiation of water crystallization [20]. Under these conditions, the mathematical reliability of f_A -approximations TDs of water characteristics and the adequacy of interpretations of the nature of molecular motions will decrease [34, 35]. However, in the supercooled state of water noise decreases and the accuracy of spectral methods increases [20]. The data on supercooled physics can be used in qualitative correlations together with data obtained under normal conditions.

In this work, to substantiate the physical nature of molecular motions and intermolecular bonds responsible for the anomalies of the properties of liquid water under normal conditions, Arrhenius approximations were applied to the known temperature dependences of the characteristics of molecular dynamics and water structure.

2. Materials and methods

The empirical data $A(T)$ for the TDs characteristics of water was taken from published works, references to them are given in the captions to the figures and in the tables. If necessary, digitized graphs with the use of 'Paint' computer application. The borders of the entire temperature range for TDs were defined based on those of available data varying in the limits T of -30 °C to 100 °C. On the f_A -approximation graphs, junction points of adjacent T intervals were marked with arrows. 'MS Excel' application was used to plot TDs and its f_A -approximations. The extent of proximity of value R^2 to 1 was chosen as reliability criterion for f_A -approximations, in various T intervals. The error in the calculation of activation energies was determined by the accuracy of the calculated or experimental TD characteristics of water and its structural parameters. Characteristic deviations of the values are given in the tables.

In work [5], mathematically reliable and physically adequate in certain T intervals f_A -approximations dependences of water characteristics on $1/T$ were obtained:

$$f_A = \exp(\pm E_A/RT), \quad (1)$$

where R is specific gas constant ($8.3 \text{ J mol}^{-1} \text{ K}^{-1}$), and the effective E_A indicated the thermal effect ($\pm \Delta Q$) of the reaction of the rearrangement of the water structure, the sign of which depends on the type of reaction (endo or exo). The Arrhenius exponent in (1) in the general case will be a bimodal function, reflecting the dependence of TD on two types of thermodynamics [8, 24]:

$$TD = F_T(T) F_R(T), \quad (2)$$

where $F_T(T)$ represents the dependence of all types of molecular motions on thermal energy (Q) and obeys the Boltzmann distribution, and Q integrates the entire spectrum of energy quanta corresponding to the equilibrium radiation of the body at T. $F_R(T)$ represents the dependence of TD on the thermodynamics of reactions that limit the configuration adjustment at the SMS level. The $F_T(T)$ function in [5] was modeled by a power function:

$$F_T(T) \propto T^\beta.$$

The value and sign of β for each macro characteristic of water should satisfy the known relations between them and the physical correlations between the macro and micro characteristics of water. For translational and rotational self-diffusion of water under normal conditions, the Stokes-Einstein ratio is valid:

$$D\eta \propto T,$$

The viscosity depends on the energy and the number of HBs per average molecule and therefore TD η will obey the Boltzmann distribution with $E_A = E_H$. It allows to take $\beta = 0$ for η , τ_D , and T_1 , and $\beta = 1$ for D. For water as an equilibrium thermodynamic system, the following relations are valid:

$$P_V \propto T \text{ and } v = \mu\rho^{-1},$$

(μ - the molar mass of water) taking into account the expansion of bodies with increasing T for v and the radii of the peaks $g_{oo}(r)$ we took $\beta = 1$, and for the water density (ρ) $\beta = -1$. Moreover, TD P with $\beta = 0$, similarly to TD η , must obey the Boltzmann distribution for the energy HBs.

Changes in local water density are estimated by amplitudes of $g_{oo}(r)$ peaks [9, 16]. Therefore, for TD $g_{oo}(r)$, we can take $\beta = -1$ and, taking into account $\beta = -1$ for ρ , calculate the values of β for TD γ and V, using the well-known relationships [7, 9]:

$$V = (\gamma \rho)^{-1/2}.$$

For γ and V the values $\beta=2$ and -0.5 [5] were suitable, respectively. The C_P value is determined by the number of degrees of freedom, which directly depends on T , so for the analysis of its TD we used $\beta=1$ [5]. Assuming that the transfer of energy of elastic oscillations is responsible for the propagation of heat in liquids, the formula for the coefficient of thermal conductivity (κ) was obtained [33]:

$$\kappa \propto \frac{C_p \rho^{4/3}}{\mu^{1/3}}$$

from which it follows that $\beta = -1/3$ for κ . In the analysis of TD, the water refractive index (n_D , $\lambda = 589$ nm) was taken to be $\beta = -1$, based on the fact that ε depends on T^{-1} [9, 29].

Thus, using the well-known laws of molecular physics to substantiate the value of β , for each characteristic of water it is possible to construct a physically adequate and mathematically reliable f_R -approximation of its TD.

According to (2), f_A -approximation is a bimodal function of $1/T$:

$$f_A = f_T f_R,$$

The explicit form of the function f_R can be obtained by representing f_T -approximation T^β in the form:

$$f_T = \exp(\pm E_T/RT),$$

where the plus sign corresponds to $\beta < 0$, and the minus sign for $\beta > 0$. Then for f_R we get:

$$f_R = f_A/f_T = \exp(\pm E_A/RT)/\exp(\pm E_T/RT) = \exp[(\pm E_A \pm E_T)/RT] = \exp(\pm E_R/RT),$$

$$\pm E_R = \pm E_A \pm E_T.$$

The contribution of the configurational component to the TDs of the static characteristics of water is likely to be comparable with the thermal component and insignificant for dynamic characteristics. Correspondingly, this will manifest itself in the ratios of E_R , E_A , and E_T .

The E_R values can be used to characterize the type of movements that are mainly responsible for configuration changes in SMS. They make a large contribution to C_P [9] and this confirms the low reliability of f_A in Fig. 2b. Given that TD for C_P is proportional to T ($\beta = 1$) [5], E_R was determined from the f_R -approximation of C_P/T values (Fig. 2c). In Fig. 2d shows f_T -approximation $F_T(T) = T$. Multiplying by R the numbers in the exponents f_R , f_A and f_T , we get the values of E_R , E_A and E_T in J/mol. For example, E_R for $t > 36$ °C $E_R = E_A - E_T = -16 - (-339) = 323$ (2.68 kJ/mol) and for $t < 36$ °C $E_R = 20 - (-290) = 310$ (2.57 kJ/mol) Trends f_R intersect at the point $t_E = 35.7$ °C

(Fig. 2b). The values of E_R , E_A , and E_T are determined in a similar way for other characteristics of water at nonzero values of β .

Rotational and translational movements of molecules in liquid water occur in the fields of nearby and distant neighbors, this causes the effect of inhibition (friction [9]). Excessive external pressure (P^+) enhances the effect of inhibition and affects the TDs of water characteristics [7, 17, 36-40]. The magnitude of the inhibitory effect of P^+ will depend on the value of P^+ and the energy of molecular motion. To evaluate the effect of P^+ , we determined the f_A -approximations TDs of a number of water characteristics obtained for different P^+ . To estimate the distances between ions and molecules in water, we used the formula [41] :

$$L = 11.8 C^{-1/3} \text{ \AA},$$

where C is the concentration in mol/l. For pure water, $C = 55.6$ mol/l and $L = 3.1$ \AA, which is close to the radius of the first coordination shell $r_{00} = 2.8$ \AA [9].

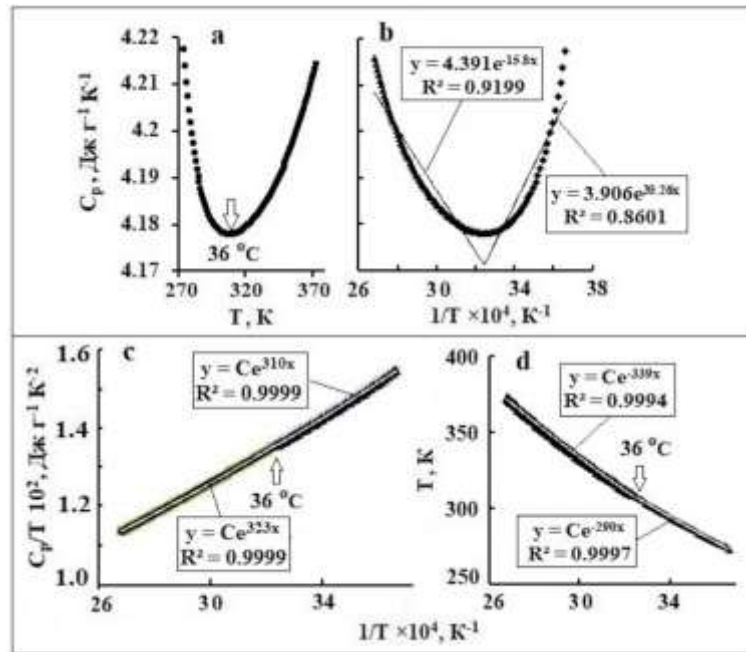


Fig. 3. Temperature dependence of water specific heat capacity (C_p) on T (a); f_A -approximation (b), f_R -approximation (c). Data on C_p were imported from [5, 8]. (d) The dependence of T on $1/T$ and its f_T -approximation. Lines of trends are colorless.

3. Results

Graphs of TDs of water characteristics, as well as TDs of structural and spectral parameters together with their f_A -approximations are shown in Fig. 3 - 17. Extreme points (t_E °C), parameters

β , E_A , E_T , E_R of the functions f_A , f_T , f_R for micro characteristics are presented in Table 1, and for macro characteristics in Table 2.

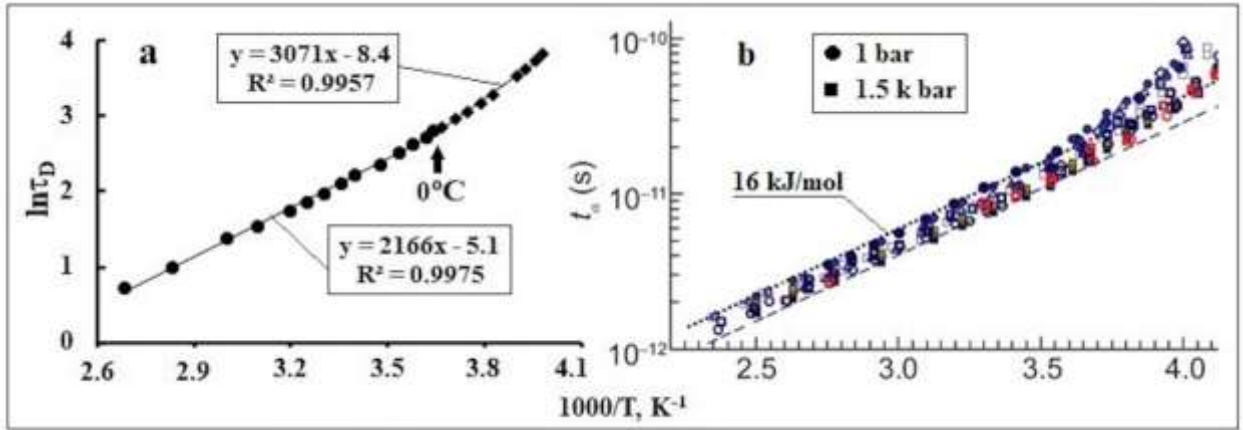


Fig. 4. (a) f_A -Approximation for TD of water dielectric relaxation time ($\ln \tau_D$), initial data from [5, 29]. (b) Arrhenius dependence of the hydrogen bond lifetime (t_a) and the characteristic times of dynamic processes in liquid water at different pressures, obtained by NMR (Figure from [43]).

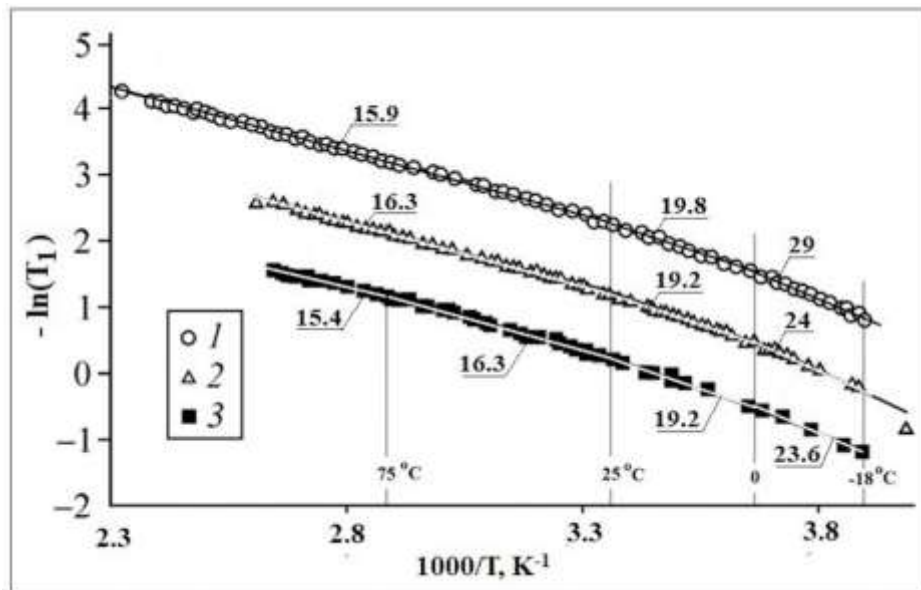


Fig. 5. Arrhenius dependences of the spin-lattice relaxation time (T_1) and their f_A -approximations (lines of trends are colorless); 1 - distilled water, 2 - seawater (~ 0.6 mol/l NaCl), 3 - NaCl solution (0.5 mol/l). Adapted figure from [44].

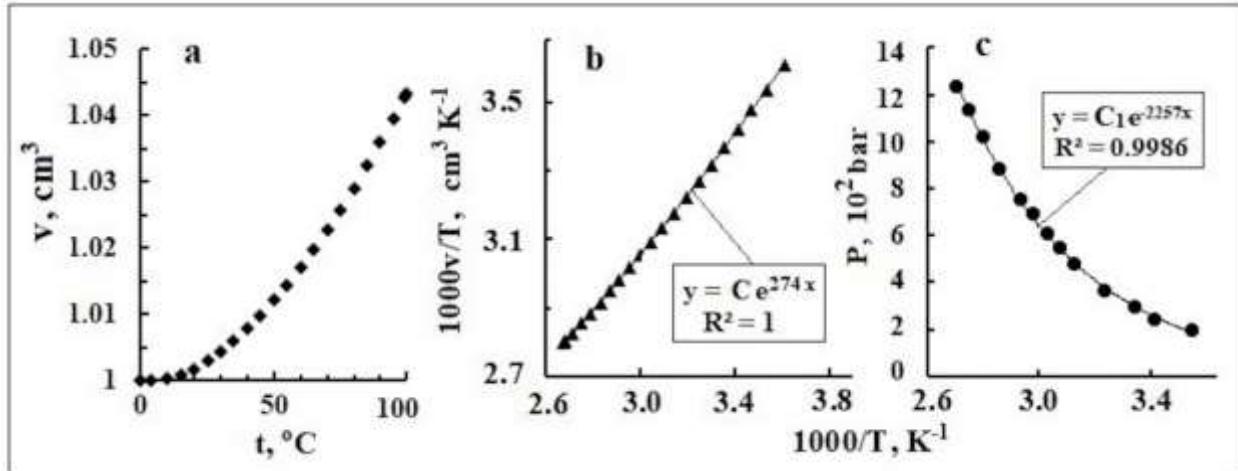


Fig. 6. (a) Temperature dependence of water specific (molar) volume (v); (b) its f_R -approximation. (c) Pressure (P) versus $1/T$ at a constant specific volume (0.99 cm³g⁻¹) and its f_A -approximation. Initial data for v and P from [7].

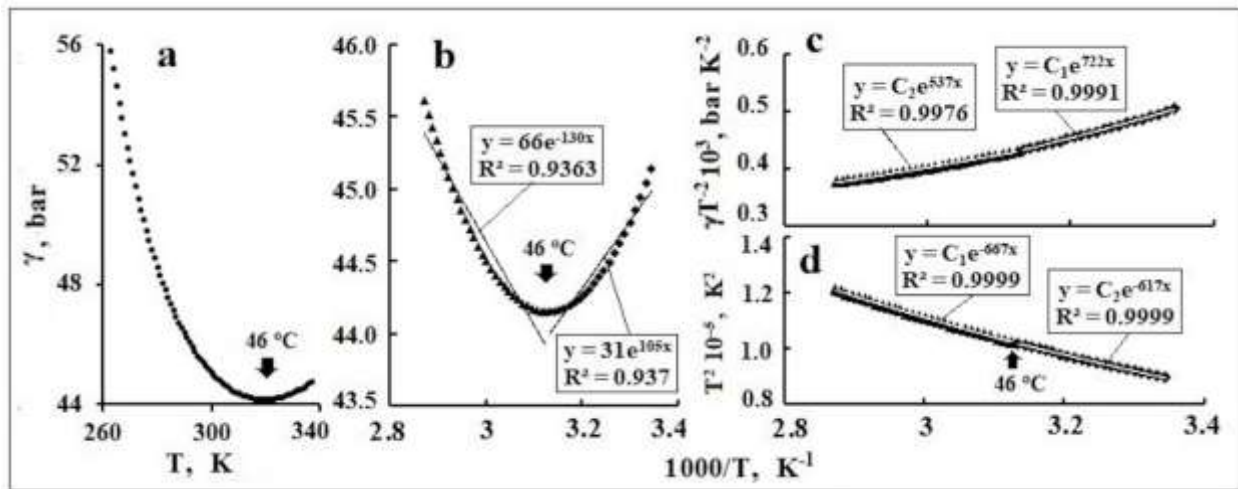


Fig. 7. (a) Temperature dependence of compressibility (γ); (b) its f_A -approximation and (c) f_R -approximation; (d) T^2 on $1/T$ and its f_T -approximations. Initial data on $\gamma(T)$ from [5]. Arrows show t_E . Lines of trends are colorless.

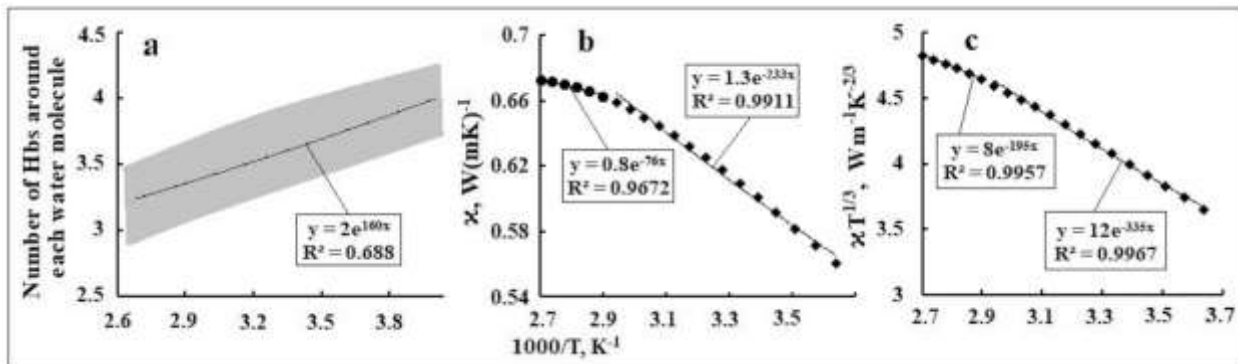


Fig. 8. (a) f_A -Approximation number of hydrogen bonds around each water molecule (Adapted figure from [7]). Dependences of the thermal conductivity coefficient (κ) (b) and κT (c) on $1/T$ and their f_R -approximations. Initial data from [45].

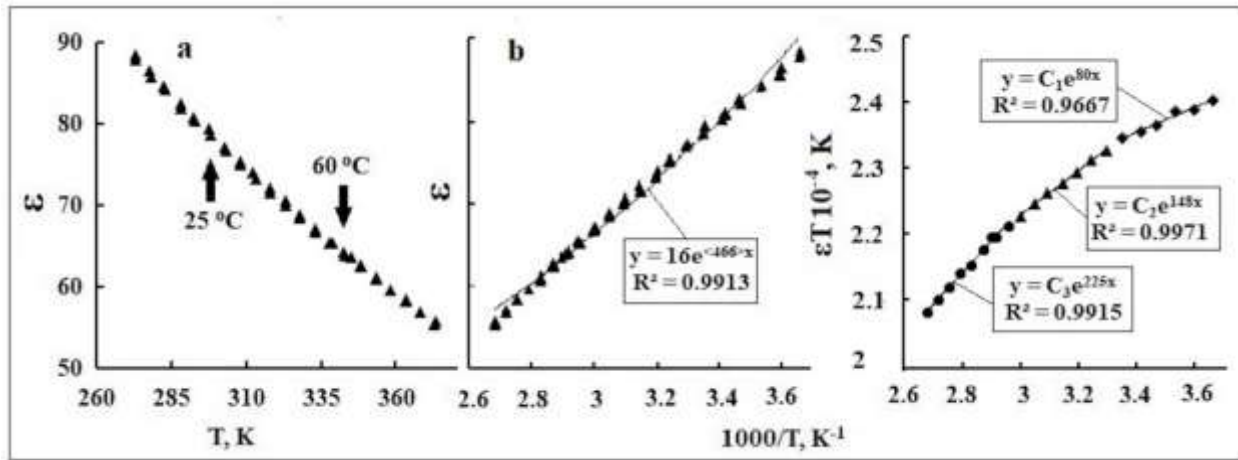


Fig. 9. Temperature dependence of the dielectric constant (ϵ) of water; (a) its f_A -approximation; (b) its f_R -approximation (c). Initial data from [9, 29, 46, 47].

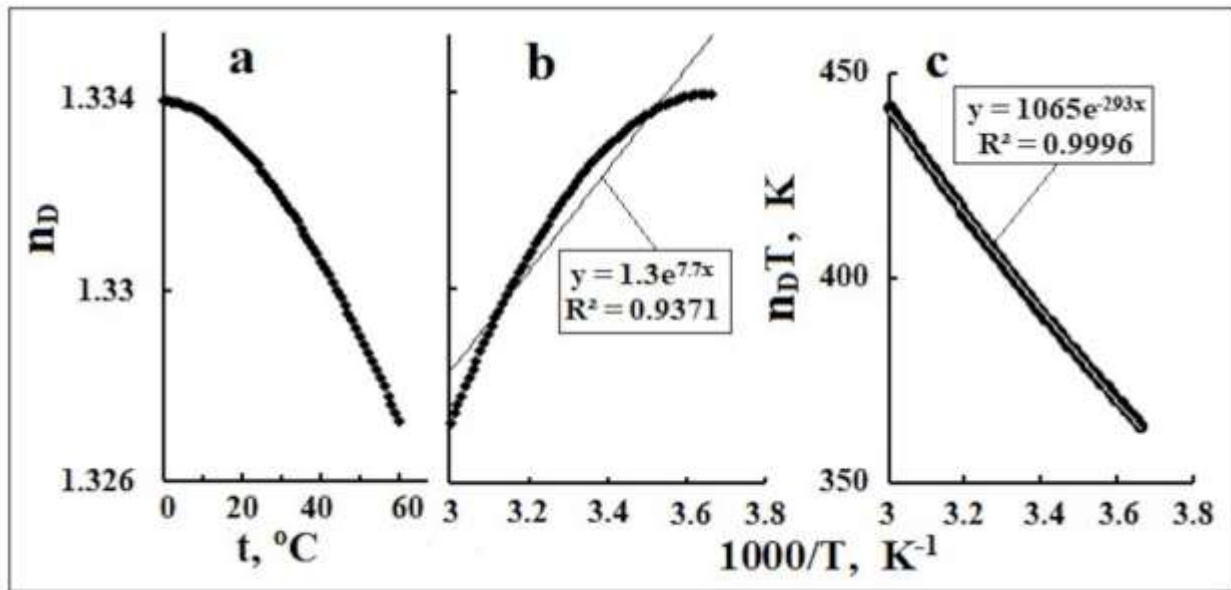


Fig. 10. (a) Temperature dependence of the refractive index of water at a wavelength of 589 nm (n_D); (b) f_A -approximation; (c) f_R -approximation. Initial data from [48].

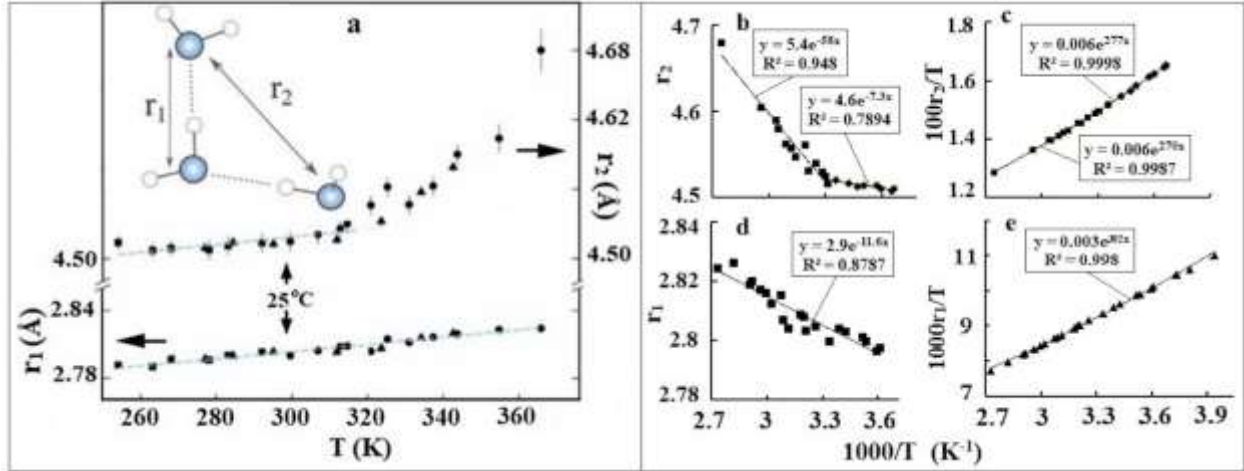


Fig. 11. (a) Temperature dependence of the first (r_1) and second (r_2) peak in $g_{00}(r)$ function from neutron scattering D₂O; (b), (d) their f_A -approximations; (c), (d) its f_R -approximations. Adapted figure (a) from [19].

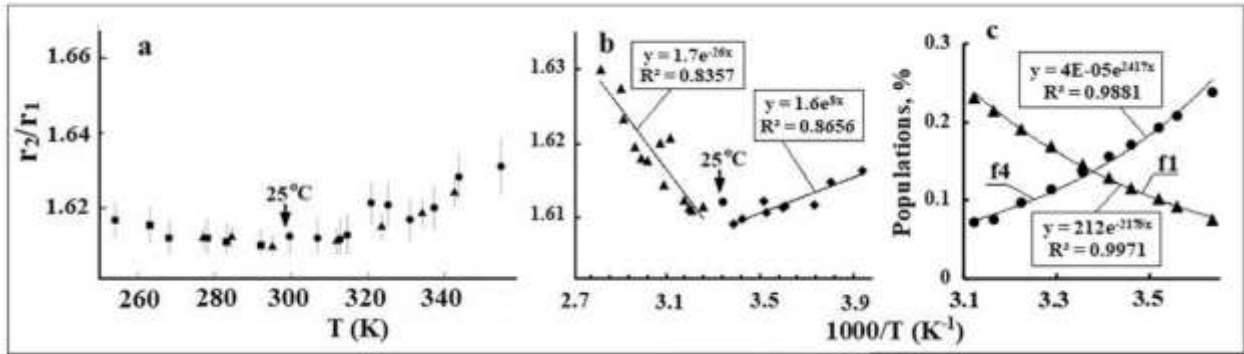


Fig. 12. (a) Temperature dependence of the relations first (r_1) and second (r_2) peak in $g_{00}(r)$ for D₂O (r_2/r_1); (b) its f_A -approximations. Adapted figure (a) from [19]. (c) Temperature evolutions O-H stretching modes of populations f_1 (the shoulder 3620 cm⁻¹) and f_4 (the shoulder 3260 cm⁻¹) and their f_A -approximations. Initial data from [26].

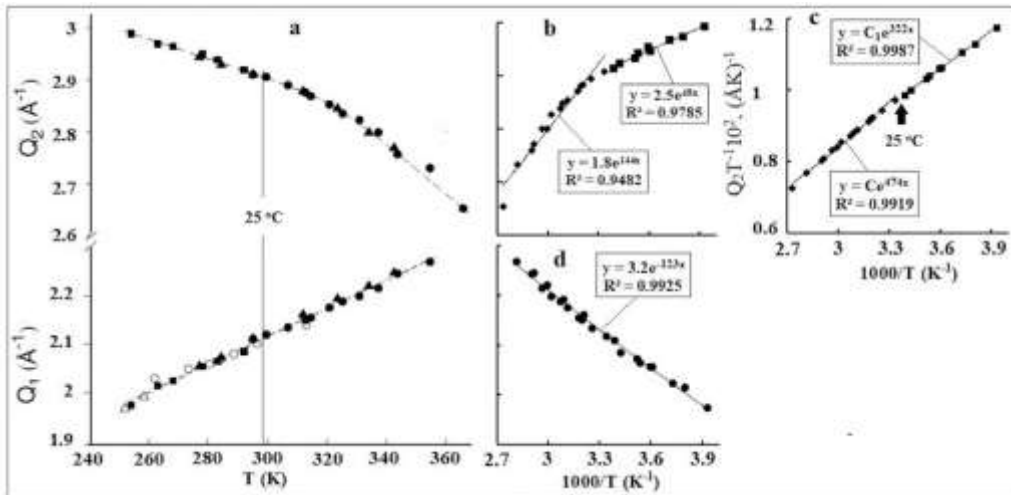


Fig. 13. (a) Temperature dependence of the first Q_1 (\AA^{-1}) and second Q_2 (\AA^{-1}) peak maximum positions; (b), (d) their f_A -approximations; (c) f_R -approximation. Adapted figure (a) from [15, 19, 21].

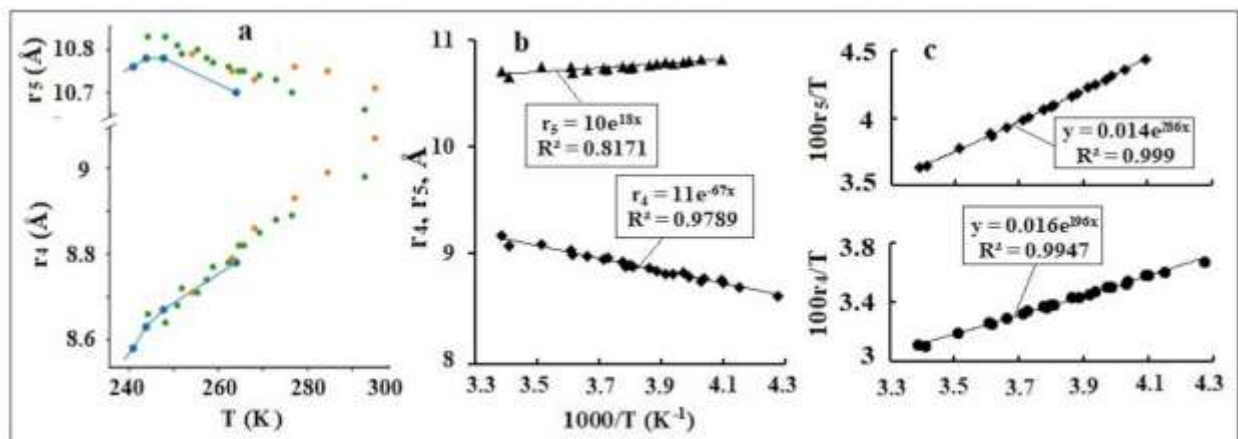


Fig. 14. (a) Peak location of the 4th ($r_4 \sim 9 \text{\AA}$) and of the 5th peak ($r_5 \sim 11 \text{\AA}$) of $g_{oo}(r)$. (b) Their f_A -approximations and (c) f_R -approximations. Adapted figure (a) from [35].

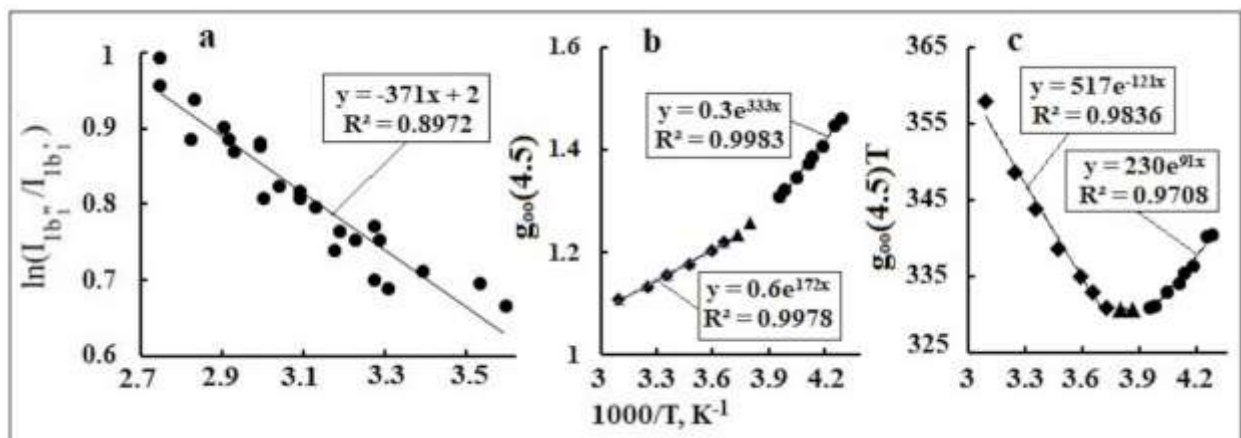


Fig. 15. (a) The temperature dependence of the logarithm of intensity ratio of bands 1b'' (distorted) and 1b' (tetrahedral) of peaks in the lone-pair region of O in x-ray emission spectra of D_2O and its f_A - approximation. Adapted figure from [12]. (b) f_A -Approximation TDs amplitude of peak $g_{oo}(4.5 \text{\AA})$; (c) its f_R -approximation. Data x-ray scattering H_2O from [21].

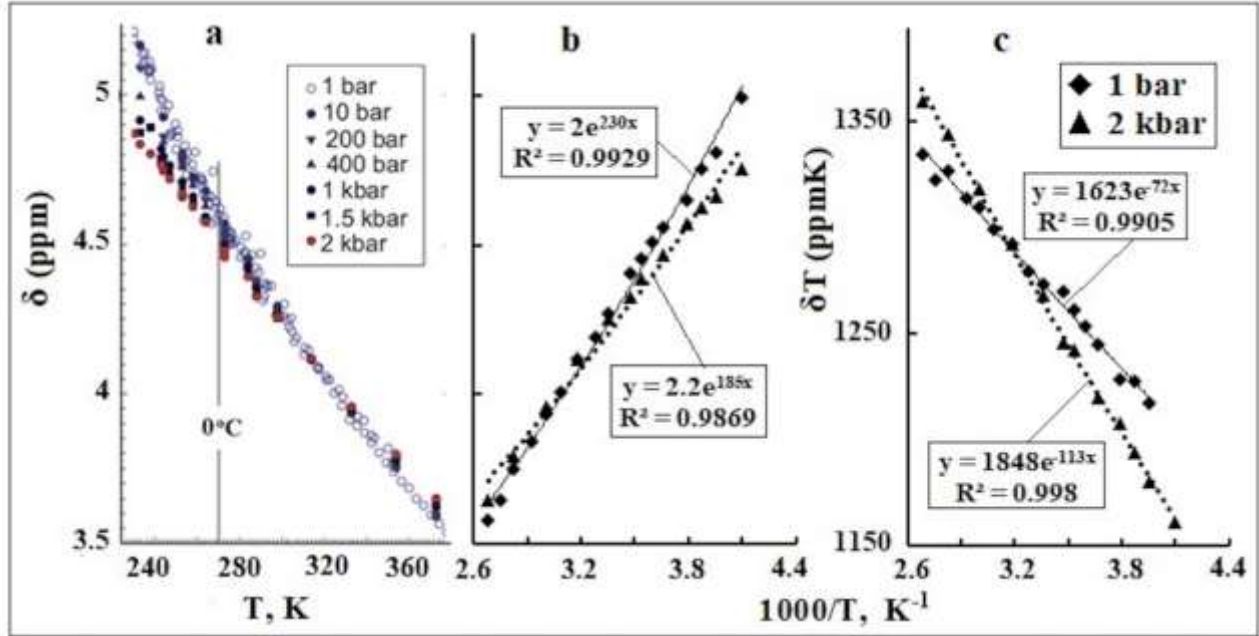


Fig. 16. (a) TD chemical shift (δ) H_2O at different pressures; (b) their f_A -approximation; (c) their f_R -approximation. Adapted figure (a) from [43].

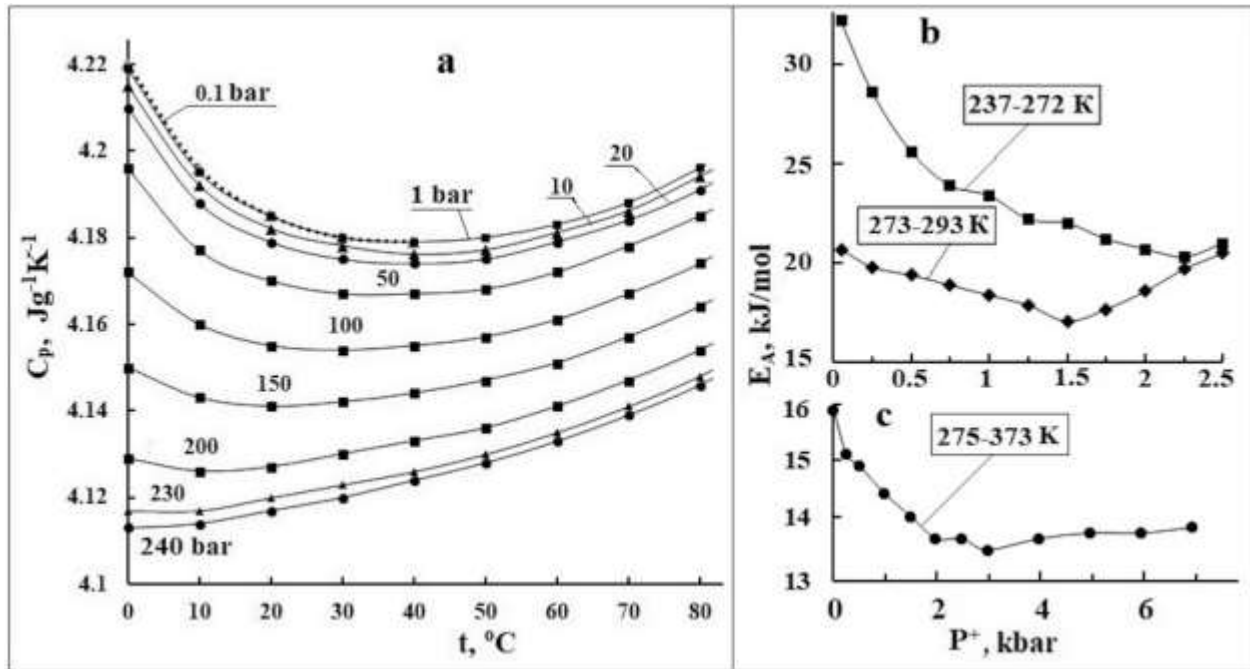


Fig. 17. (a) Temperature dependence of the adiabatic heat capacity (C_p) at an external pressure P^+ from 0.1 bar to 240 bar. (b) Pressure dependence of activation energy (E_A) of spin-lattice relaxation (T_1) in two ranges of T . (c) Pressure dependence of E_A of shear viscosity (η). The initial data (a), (b), (c) from [39], [40], [9], respectively.

Table 1

Extreme points and activation energy of the temperature dependences of the water spectral and structural characteristics.

Spectral and structural parameters		β	t_E	Δt	E_R	E_A ($E_R + E_T$)	Fig. N; [Ref]	
								°C
ν_{OH} (cm^{-1})	3260	0	-	-2 – 47	-18		12	
	3620				20			
$Ln(1b''/1b')$		1	-	4 – 90	3.0		15	
r_{OO} (Å)	2.8				1	25		-19 - 93
	4.5	0 – 25	2.3	-0.06				
		29 – 91	2.2	-0.48				
	~9	-	-29 – 22	0.8			2.8	
~11	-1.0			1.4				
Height g_{oo} (4.5 Å)		-1	-12	-40 – -15	1.6	-0.6	15	
					0 – 50	2.4		0.15
Q_1 (Å ⁻¹)		0	-	-20 – 93	-1.0		13	
Q_2 (Å ⁻¹)		1	25	-20 – 22	2.7±0.3	0.4±0.1		[15, 19, 21]
				26 – 93	3.9	1.2		

4. Discussion

The physical adequacy of f_A -approximations for the dynamic characteristics of water (D , η , τ_D , P , ν_{OH}) in the T-interval 0-100 °C is evidenced by the correlation of the values of E_A (Table 2) with the value of $E_H = 19 \pm 12$ kJ / mol [9, 25]. This result confirms the assignment of dynamic characteristics TDs to I-type thermodynamics. The dynamic characteristics TDs at $T < 273$ K become non-linear (Fig. 5; Fig. 11-14, Fig. 16) and the reliability of f_A -approximations in the T-interval of -30–0 °C decreases. In this case, E_A values increase, remaining less than the absolute value of the maximum value of E_H . This indicates an increase in E_H and friction forces in the dynamics of supercooled water.

A feature of molecular physics of compressibility (γ), sound vibrations (V) and dielectric properties (ϵ) of water is the limitation of the isotropic dynamics of molecules by motions directed along the action vector of an external force. In the case of γ and V , this is a mechanical factor similar to P^+ , and in the case of ϵ , it is the local Coulomb forces in the domains of polarized dipoles. In isotropic self-diffusion (translational and rotational) 6 degrees of freedom are equivalent [9] and, accordingly, 6 components of E_A , which have close values for D , η and τ_D (Table 2, [9]).

Table 2

Extreme points, parameter β and activation energy of Arrhenius approximations of the temperature dependences of the water characteristics.

Fig. N, [Ref]	Water characteristics		β	t_E	Δt	E_T	E_R	E_A ($E_R + E_T$)					
				°C		kJ/mol							
[5]	D (cm ² s ⁻¹)		1	0;	-30 – 0	-2.2	-27.8	-30					
				25	0 – 25	-2.7	-	-20.2±0.3					
					26-100	-2.8	-	-16.8±0.4					
[5]	η (cP)			0;	-10 – 0	-2.6	22.4						
				25	0 – 25		19.0±0.3						
					25 – 100		14.0						
4	τ_D (s)		0	0	-13 – 20		25.6 [29]						
					-22 – 0		25.5						
					2 – 100		18						
6	P (bar)		0	-	9 - 97		-18.7						
9	ε		-1	25;	0 – 25	2.4	0.66	3.1					
				60	30 – 60	2.6	1.2	3.8					
					65 – 100	2.9	1.8	4.5					
8	κ (Wm ⁻¹ K ⁻¹)		1/3	~72	2 – 67	-0.8	-1.9	-2.8					
					72 – 97	-1	-0.6	-1.6					
[5]	ρ (kg m ⁻³)		-1	0;	-30 – 0	2.1	-2.4	-0.3					
				4	0 – 3	2.28	-2.31	-0.03					
					4 – 100	2.7	-2.3	0.4					
6	v (cm ³ mol ⁻¹)		1	4	4 – 100	-2.65	2.28	-0.37					
3	C_p (J g ⁻¹ K ⁻¹)		Ice	0	-	-93 – -3	-	-1.8					
					Water	1	0;	-27 – 0	-2.1	4.5	2.4		
							36	0 – 36	-2.4	2.57	0.17		
[7, 39]	Water		1	36	37 – 100	-2.81	2.68	-0.13					
					[5]	V (m s ⁻¹)		-0.5	25;	0 – 25	1.1	-2.9	-1.8
									46;	26 – 46	1.3	-2.3	-1.0
75	47 – 75	1.38	-1.73	-0.35									
	76-100	1.49	-1.14	0.35									
[7]	γ (bar ⁻¹) [5]		2	0;	-30 – 0	-4.4	10	5.6					
				25;	0 – 25	-4.7	7.9	3.2					
				46;	26 – 46	-5.1	6	0.9					
				75	47 – 75	-5.5	4.5	-1.0					
					76 – 100	-6.0	3.1	-2.9					
16	δ (ppm)	1 bar	-1	-	-29 – 100	-2.5	-0,6	1.9					
		2 kbar				-2.4	-0,9	1.5					
10	n_D			-	0 – 60	2.5	-2.44	0.06					

Obviously, for TDs γ , V , and ε , motions and intermolecular interactions are collinear to the external force vector. Indeed, the quantities $|E_A/6|$ for D , η and τ_D correlate with $|E_A|$ for γ , V , ε in the range of 0-25 °C far from the vicinity of t_E γ , V (Table 2).

The ratio $E_A^Y \sim 2E_A^V$ is consistent with the periodicity of the external force, causing a reversible compression of the water structure. From the relation $E_A^D/6 \sim E_A^X$ (Table 2) it follows that the directed flux of IR quanta acts on the water dynamics anisotropically similar to acoustic waves. The value of δ , in contrast to the kinetic characteristics of τ_D and T_1 , depends on the degree of screening of the magnetic field on the central molecule by the local magnetic fields of the electrons of the near shells. This dependence will be sensitive to the direction of the constant magnetic field and depend on T similarly to TD ε . In this case, the ratio $E_A^\delta \sim E_A^\varepsilon/2$ can be related to the difference in the orientation effects of the orbital moments of electrons and dipole moments of molecules. Thus, it can be said that in the range of 0-25 °C the features of TDs of conditionally static characteristics (γ , V , ε , κ , δ) and dynamic characteristics have the same nature. However, at $0 < t < 100$ °C, the E_A values of these characteristics, similarly to E_A for ρ , v , C_p and n_D , become significantly lower than E_H (Table 2), therefore, the mechanism of their TDs anomalies must obey type II thermodynamics.

The nature of the movements responsible for the TDs characteristics of water should be manifested in qualitative correlations between the E_A values for macro and micro characteristics of water (Table 3). The qualitative level of correlations is primarily due to weak TDs of water structure parameters [9, 22] and large scatter of points in TDs obtained by different methods and authors [34] (Figs. 8a, 11a, 13a, 14a, 15a, Table 1). In the structure of the second coordination shell $r_{oo} = 4.5$ Å at $t < 25$ °C molecules with tetrahedral HBs [13, 15], which are part of the ice-like W_6 clusters, predominate. The W_6 transformation during the transition of LDL to HDL in the vicinity of $t_E = 4$ °C is associated with the entry of free molecules into their voids and leads to a change in the number of molecules in the second coordination shell. This rearrangement can be associated with the extrema at TDs ρ and v , as well as the kink f_A -approximation of g_{oo} (4.5 Å) in the region of -15-0 °C (Fig. 15b). The value of E_A for superlattices correlates with the E_A of all molecular motions with $E_A < 3$ kJ/mol and in all structural shells. TD n_D can be attributed to TDs of the polarization of molecular dipoles in shells with $r_{oo} = 2.8$ Å and $r_{oo} = 4.5$ Å, which is sensitive to the electric component of light with $\lambda = 589$ nm and this indicates the long-range and speed of

the inductive polarization SMS. The magnitude of the E_A chemical shift (δ) correlates with the energy of proton motions of all coordination shells.

Table 2

Compliance E_A micro and macro characteristics of liquid water

Micro characteristic			Macro characteristic								
Parameters	Δt (°C)	$ E_A $ (kJ/mol)	ε	κ	ρ	v	C_p	V	γ	δ	n_D
r_{oo} (Å)	2.8	-19 - 93	0.1					+			+
	4.5	0 - 25	0.06			+	+	+			+
		29 - 91	0.48			+	+	+	+		
	~9	-29 - 22	2.8	+	+			+		+	+
	~11		1.4					+	+	+	+
g_{oo} (4.5 Å)	-40 - -15	0.6			+	+					
	0 - 50	0.15			+	+	+				+
Q_1 (Å ⁻¹)	-20 - 93	1.0						+	+	+	
Q_2 (Å ⁻¹)	-20 - 22	0.4			+	+					
	26 - 93	1.2		+				+	+	+	

The E_A value in the range 0–25 °C is 3.1 kJ/mol (Table 2) for the stationary dipole moment of water (ε) modulo close to $E_A = -3$ kJ/mol for $\ln(1b''/b')$ (Fig. 15a). According to the data of [10, 12, 17] $E_A'' \gg E_A'$, therefore -3 kJ/mol can be attributed to the endothermic reaction of molecule rotation in the field of delocalized HBs. It is believed that the tetrahedral configuration of LDL water transforms into the distorted configuration of HDL water [17, 22]. Motions of this kind can occur in concert with exothermic reactions of reorientations of dipoles and limit TD ε . The kinks TDs D , η , τ_D , V , γ , ε (Table 2) in the vicinity of 25 °C correspond to kinks at this point TDs of the parameters of the second coordination shell - Q_2 (Å⁻¹) and r_{oo} (4.5 Å), as well as the minimum TD ratios r_2/r_1 (Fig. 12b). These results confirm the hypothesis of spasmodic transformation in the vicinity of the 25 °C point of the ice-like cluster W_6 in the LDL in HDL phase transition [5, 8, 11, 13, 22].

Under normal conditions, E_A values for T_1 of seawater remain practically unchanged, while in its supercooled state E_A increases only 1.2 times, while in supercooled ordinary water it is 1.5 times (Fig. 5). For seawater ($C_{NaCl} \sim 0.6$ mol/l) with a uniform distribution of Na and Cl ions, Eq. (2) implies $L \sim 11$ Å; therefore, the effects of ion hydration can only slightly affect the dynamics of the fifth coordination shell (Table 1). It follows that the TDs of the properties of physiological

fluids ($C_{\text{NaCl}} \sim 0.16 \text{ mol/l}$) at $\sim 40 > t > 0 \text{ }^\circ\text{C}$ will be the same as for pure water. In electrolytes ($C_{\text{NaCl}} \sim 4 \text{ mol/l}$), the distance between ions $L \sim 6 \text{ \AA}$ and hydration effects are comparable with the action of high P^+ and lead to significant changes in the pair distribution functions of the first and second coordination shells [37, 38]. Accordingly, the reliability of f_A approximations of the TDs properties of electrolytes will decrease as well as for supercooled water.

Pressure as a thermodynamic characteristic is proportional to T , but E_A obtained from its TD at $v = \text{const}$ is ~ 7 times larger than E_T (Fig. 6, Table 2). This is consistent with the assignment of P to the dynamic characteristics for which $E_A \gg E_T$. External overpressure (P^+) is a mechanical factor that generates stresses, shifts and deformations in the volume of water. Under the influence of P^+ , the threshold of excitation of molecular movements decreases and the effect of friction is simultaneously enhanced. As a result, the values of T_E and E_A decrease, and the more, the higher P^+ and less E_A (Fig. 17). High values of E_A for dynamic characteristics neutralize the P^+ effect in the region $t > 0 \text{ }^\circ\text{C}$ (Fig. 4b) and the difference in the effect of P^+ on their TDs is manifested only in the positions of the minimum dependences of E_A on P^+ – 1.5 kbar for T_1 and 3 kbar for η (Fig. 17). It can be assumed that in the vicinity of the E_A minimum, the threshold and inhibitory effects of P^+ are compared and, with a further increase in P^+ , the prevailing inhibition effect leads to an increase in E_A . In supercooled water, both the inhibition effect and E_A increase. It is known [49] that the effect of high P^+ on translational diffusion (D and η) is much stronger than on rotational (τ_D and T_1). This explains the shift of the E_A minimum at T_1 from 1.5 kbar in ambient water to 2.25 kbar in supercooled water (Fig. 17b). Note that, depending on $r_{00}(2.8 \text{ \AA})$ as a function of P^+ , a minimum is also observed at ~ 2 kbar [7].

Estimates of E_A for static characteristics obtained from Fig. 16, Fig. 17a and [7, 36, 39] and showed that E_A slightly decreases in the interval $0 < t < 100 \text{ }^\circ\text{C}$ with an increase in P^+ up to 2 kbar (Table 2). The nature and energetics of the molecular motions responsible for the TDs anomalies of these characteristics correlate with the signs and magnitudes of T_E shifts for the corresponding P^+ ($\Delta T, P^+$): C_p (-36K, 200 bar) (Fig. 17b); ρ (-33K, 1 kbar,) [7]; V (20K, 2 kbar) [7]; and γ ($\sim 0\text{K}$, ~ 2 kbar) [36].

The molecular mechanism of the TDs C_p , ρ , V , and γ anomalies is, in fact, close to the physics of homogeneous crystallization of water at $0 \text{ }^\circ\text{C}$. The thermodynamics of these processes covers the entire volume of water, the values of Q and E_A before and after T_E have different signs, at extremes $E_R = E_T$ and $E_A = 0$. The kinks TDs of dynamic characteristics at a point of $25 \text{ }^\circ\text{C}$

indicate the completion of the decomposition of Ih ice structures. A key moment in the physics of water crystallization at 0 °C and atmospheric pressure is the exothermic chain reaction of W_6 binding in active centers to network structures (SMS*) preceding the ice structure Ih. The main feature of the active center is the inhibition of reverse SMS* decay reactions by removing the thermal effect of the crystallization reaction ($Q = 6$ kJ/mol) outside the nucleation centers. An energy of 6 kJ/mol corresponds to one IR quantum $\omega = 500$ cm⁻¹ or two with a frequency of 250 cm⁻¹ (Fig. 1).

An effective removal of Q occurs in microdroplets of water in the experiment [15, 50] and in the formation of snow in the atmosphere, as well as in the presence of impurities reradiating IR quanta (250 cm⁻¹ or 500 cm⁻¹) in the transparency windows SMS*. By analogy with the HDL → LDL phase transition, the SMS* formation mechanism was presented as follows. In each cluster of the coupled pair W_6 , mirror-symmetric anomeric rotations with $E_A \sim 3$ kJ/mol, coupled with the relay reaction of the occurrence of HB with W_6 in the adjacent pair, occur in concert. SMS* was called the metastable phase “ice 0” and determined that each layer is a mirror image of the previous layer [51]. When ice is heated from 0 °C to 4 °C, the reverse endothermic reaction LDL → HDL starts, which is accompanied by the transformation of cells in SMS* layers. In this case, voids arise and free molecules enter into them, while the bulk density of the SMS* phase becomes maximum, and the specific volume is minimal. Further heating above 4 °C initiates the decay of SMS* into W_6 "monomers" and this process is mostly completed in the vicinity of 25 °C.

At the points t_E TDs ρ (v), C_P , γ , V the value $E_A = 0$ due to the fact that E_T and E_R are equal in modulus and have different signs (Table 2). Under such conditions, isoenergetic phase transitions of the second kind occur, in which only the SMS conformation changes [24]. At the minima TDs C_P and γ for $t < t_E$ $|E_R| > |E_T|$ and $E_A > 0$ (exo), at $t > t_E$ $|E_R| < |E_T|$ and $E_A < 0$ (endo). At the maxima, TDs ρ and V for $t < t_E$ $|E_R| > |E_T|$ and $E_A < 0$ (endo) for $t > t_E$ $|E_R| < |E_T|$ and $E_A > 0$ (exo). The signs of the thermal effect and the value of the extremum are determined by the signs of β and the ratio of the values of R_T and Q of the SMS rearrangement reaction.

Points t_E for static characteristics are critical points, similar to Curie points of liquid-crystal ferroelectrics [52]. It is believed [30] that at the critical point, the amplitude of long-wavelength fluctuations of the order parameter increases so much that they become independent of microparameters that regulate short-range intermolecular interactions. In this case, the fluctuations activate the resonant transitions in the macrosystem of energetically coherent states and a new

stable or metastable phase arises in SMS. The boundaries of the critical region are determined by the ratio $(T - T_E)/T_E \approx 10^{-2}$, which is performed for the T_E points of the extrema TDs ρ , C_P , γ , and V . The structure of the water is rearranged in the interval $|T - T_E| \sim 4$ K, in which E_A remains close to zero (e.g. ρ in Table 2).

The phase transition at the Curie point of a liquid ferroelectric is associated with a spontaneous polarization process, the possibility of which in water is due to the proximity of the energy van der Waals interactions with the values of E_H and E_A for ϵ and τ_D (Table 2). Spontaneous polarization effects can be associated with a ~ 1.6 -fold increase in the dipole of a molecule in a volume as compared with a dipole of a free molecule equal to 1.85 D [6, 9, 53, 54]. An adequate order parameter in liquid water is the orientation of classical Drude oscillators [53], whose frequencies at T_E points will correspond to the molecular oscillations that dominate the SMS restructuring. According to Wien's law, these oscillations will correspond to the frequency of the IR quantum (ν_E):

$$\nu_E \approx 5.9 \cdot 10^{10} T_E \text{ (Gz)},$$

and for t_E °C (4, ~ 25 , 36, 46, 75) the values of ν_E will be of the order of ~ 18 THz, and the oscillation period will be ~ 55 fs. Water absorption in the terahertz range at ~ 200 cm^{-1} is attributed to the first-shell dynamics, whereas a concerted motion involving the second-shell contributes most significantly to the absorption at ~ 80 cm^{-1} and ~ 2.4 THz [55]. The time of selective relaxation mode at 10 cm^{-1} (~ 0.12 kJ/mol) is 1.4 ps at 298 K [56]. The lifetime of HBs in various SMS configurations varies from 80 fs to 30 ps [24, 57]. All these movements will be answered by the corresponding Drude oscillators. Their fluctuations can be synchronized and cooperate at T_E points according to the resonance mechanism under the influence of long-wave fluctuations in the frequency of O–H bond vibrations (ν_{OH}) [8, 24, 26] (Table 1). The adoption of ν_{OH} as the main order parameter is justified by the high sensitivity of ν_{OH} to changes to the energy of a particular HB or the strength of an electric field induced on it by its neighbors [23, 26, 58-60].

5. Conclusion

Ambient water at normal pressure and temperature from 0 °C to ~ 100 °C is a solution of supramolecular structures (SMS). The lifetime, composition and degree of ordering of SMS depends on temperature. Liquid water physics combines the equilibrium thermodynamics of self-diffusion and viscosity with the thermodynamics of phase transitions between SMS conformations. The restructuring of the network of hydrogen bonds and clusters in SMS is responsible for the

extremes of density TDs (4 °C) and isobaric heat capacity (36 °C), the main static characteristics of the internal state of water. TDs of dynamic characteristics – viscosity, translational and rotational diffusion have kinks in the vicinity of 25 °C. The change in molecular dynamics at this point is apparently due to the decay of most ice-like hexagonal clusters in the SMS. The thermal energy (E_T) at the extreme points TDs of the static characteristics is equal to the activation energy (E_R) of the movements responsible for the phase transition between SMS conformations. The extrema of the compressibility TDs and the associated sound velocity are mainly due to the reaction of water dynamics to the action of an anisotropic external factor. Excessive external pressure exerts a similar effect. The nature of the movements responsible for the SMS restructuring was confirmed by qualitative correlations of the activation energies (E_A) TDs of the macro characteristics of water and the parameters of its microstructure. Using the Arrhenius approximations, the quantities E_A , E_R , and E_T were determined, representing the thermal component TDs by the function T^β [5]. The values of β satisfied the well-known formulas for the characteristics of water. The physical adequacy of the relations between the E_A , E_R , and E_T values and the qualitative correlations between the E_A and E_R values for the corresponding macro and micro characteristics can be used as boundary conditions for the molecular dynamics simulations of phase transitions in SMS and the Drude oscillators spontaneous polarization mechanism.

References

1. S.I. Aksenov Water and its role in the regulation of biological processes. M. (2004) 212
2. P. Gunz. Developmental Approaches to Human Evolution. (2015) 261. DOI: [10.1002/9781118524756.ch11](https://doi.org/10.1002/9781118524756.ch11)
3. A. Oubre, Instinct and Revelation: Reflections on the Origins of Numinous Perception. Routledge, (2013) 316.
4. A. Kholmanskiy Dialectic of Homochirality. Preprints, (2019) 2019060012. doi: <https://www.preprints.org/manuscript/201906.0012/v1>
5. A. Kholmanskiy A., N. Zaytseva, Physically adequate approximations for abnormal temperature dependences of water characteristics. J. Mol. Liq. (2019) 275, 741–8. <https://doi.org/10.1016/j.molliq.2018.11.059>
6. B. Cabane, R. Vuilleumier, The physics of liquid water. Comptes Rendus Geoscience (2005) 337 (1-2), 159-171. <https://hal.archives-ouvertes.fr/hal-00015954/document>
7. M.F. Chaplin, Water Structure and Science. <http://www1.lsbu.ac.uk/water/index.html>.
8. A. Kholmanskiy, Activation energy of water structural transitions. J. Mol. Struct. 1089, 124-128 (2015). <https://doi.org/10.1016/j.molstruc.2015.02.04919>.
9. D. Eisenberg and W. Kauzmann, The Structure and Properties of Water. Oxford University Press (1969) 310.
10. T. Tokushima, et al., High resolution X-ray emission spectroscopy of liquid water: The observation of two structural motifs. Chem. Phys. Lett. (2008) 460, 387–400

11. A. Nilsson, L. G. M. Pettersson, Perspective on the Structure of Liquid Water. *Chem. Phys.* (2011) 389, 1-34.
12. C. Huang, et al., The inhomogeneous structure of water at ambient conditions. *PNAS* (2009) 106, 15214–15218; <http://www.biophys.ru/archive/h2o-00015.pdf>
13. J.R. Errington, P.G. Debenedetti, S. Torquato. Cooperative Origin of Low-Density Domains in Liquid Water. *Phys. Rev Let.* (2002) 89(21). 215503-1 – 3-4.
14. M.-S. Lee, et al., Far-infrared absorption of water clusters by first-principles molecular dynamics *J. Chem. Phys.* (2008) 128, 214506
15. J. A. Sellberg, et al., Ultrafast X-ray probing of water structure below the homogeneous ice nucleation temperature. *Nature* (2014) **510**, 381.
16. K. Amann-Winkel et al., X ray and Neutron Scattering of Water, *Chemical Reviews* (2016) 116(13):7570–89. DOI: 10.1021/acs.chemrev.5b00663.
17. A. Nilsson, C. Huang, L. G. M. Pettersson. Fluctuations in ambient water. *J. Mol. Liq.* (2012) 176, 2–16. <http://kkrk.chem.elte.hu/molim/lectures/III.Water.Pettersson.pdf>
18. A. Nilsson, L. G. M. Pettersson, The structural origin of anomalous properties of liquid water. *Nat Commun.* (2015) 6, 8998. doi: 10.1038/ncomms9998
19. L. B. Skinner, et al. The structure of water around the compressibility minimum. *J. Chem. Phys.* (2014) 141, 214507
20. A. Taschin, et al., Evidence of two distinct local structures of water from ambient to supercooled conditions. *Nat. Commun.* 4, 2401 (2013).
21. D. Schlessinger. Molecular structure and dynamics of liquid water. Simulations complementing experiments. Stockholm. 2015
22. Ph. Wernet, The Structure of the First Coordination Shell in Liquid Water, *Science* (2004) 304. 995-915
23. J.D. Smith, et al. Unified description of temperature-dependent hydrogen-bond rearrangements in liquid water. *PNAS*, (2005) 102(40) 14171–4. <https://doi.org/10.1073/pnas.0506899102>
24. A. Kholmanskiy, Kinetic factor of extreme temperature dependences of the properties of water. *Alternative Energy and Ecology.* (2014) 6, 66-74. <https://www.isjaee.com/jour/article/view/441>
25. M. Henry, Thermodynamics of hydrogen bond patterns in supramolecular assemblies of water molecules. *Chemphyschem.* (2002) 3(7):607-16. [10.1002/1439-7641\(20020715\)3:7<607::AID-CPHC607>3.0.CO;2-A](https://doi.org/10.1002/1439-7641(20020715)3:7<607::AID-CPHC607>3.0.CO;2-A)
26. J-B. Brubach, A. et al. Signatures of the hydrogen bonding in the infrared bands of water. *J. Chem. Phys.* (2005) 122: 184509
27. D.P. Shelton, Collective molecular rotation in water and other simple liquids. *Chem. Phys. Lett.* (2000) 325:513–6. [https://doi.org/10.1016/S0009-2614\(00\)00734-X](https://doi.org/10.1016/S0009-2614(00)00734-X)
28. R. A. Nicodemus, S. A. Corcelli, J. L. Skinner, A. Tokmakoff, Collective Hydrogen Bond Reorganization in Water Studied with Temperature-Dependent Ultrafast Infrared Spectroscopy. *J. Phys. Chem. B* (2011) 115, 5604–16.
29. J. C. del Valle, et al., Dielectric anomalous response of water at 60 °C, *Philosophical Mag.* **95** (2015) 683-690.
30. D. Yu. Ivanov, *Critical Behaviour of Non-Ideal Systems.* Wiley-VCH, 2008. 257
31. B. M. Smirnov, Clusters and phase transitions, *UFN*, **177**:4 (2007), 369–373.

32. Teixeira J, Luzar A, Physics of liquid water. Structure and dynamics, in “Hydration Processes in Biology: Theoretical and experimental approaches”, NATO ASI series, M.-C. Bellissent-Funel ed., (IOS Press, Amsterdam, 1999), 35-65.
33. A.G. Korotkikh, I.V. Shamanin, Bases of hydrodynamics and heat transfer in nuclear reactors. Tomsk, 2007. 117.
<http://portal.tpu.ru/SHARED/k/KOROTKIKH/eng/Teaching/Tab/Korotkikh.pdf>
34. T. Fransson et al., Requirements of first-principles calculations of X-ray absorption spectra of liquid water. *Phys. Chem. Chem. Phys.* (2016) 18, 566-83.
35. H. Pathak, et al. Intermediate range O–O correlations in supercooled water down to 235 K. *J. Chem. Phys.* (2019) 150, 224506; <https://doi.org/10.1063/1.5100811>
36. R. A. Fine, Millero F. J. Compressibility of water as a function of temperature and pressure. *J. Chem. Phys.* (1973) 59:5529–36.
37. A.K. Soper, M.A. Ricci, Structures of High-Density and Low-Density Water, *Phys. Rev. Lett.* (2000) 83(13) 2881
38. R. Leberman, A. K. Soper, Effect of high-salt concentrations on water structure. *Nature* (1995) 378, 364–6
39. A.A. Alexandrov, B.A. Grigoriev. Tables of thermophysical properties of water and water vapor: Directory. M: Publishing House MPEI. 1999. 168. ISBN 5-7046-0397-1
40. E. Lang, H.-D. Lüdemann, Pressure and temperature dependence of the longitudinal proton relaxation times in supercooled water to -87°C and 2500 bar *J. Chem. Phys.*, (1977) 67(2) 718.
41. A. Kholmanskiy A. Chirality anomalies of water solutions of saccharides. *J. Mol. Liq.* (2016) 216, 683-7. DOI: [10.1016/j.molliq.2016.02.006](https://doi.org/10.1016/j.molliq.2016.02.006)
42. F. Perakis, et al. Vibrational spectroscopy and dynamics of water, *Chem. Rev.* (2016) 116(13), 7590.
43. F. Mallamace, C. Corsaro, E. Fazio, et al. *Sci. China Phys. Mech. Astron.* (2019) 62: 107005.
44. N. A. Melnichenko, A. S. Vyskrebentsev, Parameters of the temperature dependence of the rate of magnetic relaxation of protons in water and its solutions including seawater. *J. Struct. Chem.* (2009) 50. 461.
45. Ramires M.L.V. et al. Standard Reference Data for the Thermal Conductivity of Water *J. Phys. Chem. Reference Data.* (1995) 24(3):1377-81. DOI: 10.1063/1.555963
46. L. M. Maestro, et al., On the existence of two states in liquid water: impact on biological and nanoscopic systems, *Int. J. Nanotechnol.* (2016) 13. 667-677
47. A.W. Marczewski, H₂O properties. (2002), <http://www.sorption.org/awm/utills/H2O.htm>
48. L. W. Tilton, J. K. Taylor, Refractive index and dispersion of distilled water for visible radiation at temperatures 0 to 60 °C. *J. Res. Natl. Bur. Stand.* (1938). 20, 419–477.
49. L. E. Bove Translational and Rotational Diffusion in Water in the Gigapascal Range, *Phys. Rev. Lett.* (2013) 111, 185901. DOI: 10.1103/PhysRevLett.111.185901
50. T.L. Malkin, et al., Structure of ice crystallized from supercooled water, *PNAS* (2012) 109 (4) 1041-5; <https://doi.org/10.1073/pnas.1113059109>
51. J. Russo, F. Romano, H. Tanaka New metastable form of ice and its role in the homogeneous crystallization of water. *Nature Materials* (2014) 13, 733–739
<https://www.nature.com/articles/nmat3977>

52. J. Hemine, et al., Dynamical Properties of Ferroelectric Chiral Liquid Crystals by Electro-Optical and Dielectric Spectroscopy. *Spectroscopy Lett.* (2008) 41, 285–291. <https://www.researchgate.net/publication/233455655>
53. G. Lamoureux, A. D. MacKerell, Jr., B. Roux, A simple polarizable model of water based on classical Drude oscillators. *J. Chem. Phys.* (2003) 119, 5185-97.
54. X. Ge, D. Lu, Molecular Polarizability of Water from the Local Dielectric Response Theory. United States: N. p., 2017. doi:10.1103/PhysRevB.96.075114.
55. M. Heyden, et al., Dissecting the THz spectrum of liquid water from first principles via correlations in time and space, *PNAS* (2010) 107(27) 12068–73. <https://doi.org/10.1073/pnas.0914885107>
56. I. M. Svishchev, A.Yu. Zassetsky, Three-dimensional picture of dynamical structure in liquid water. *J. Chem. Phys.* (2000) 112(3):1367-72. [10.1063/1.480689](https://doi.org/10.1063/1.480689)
57. C. J. Fecko, et al. Ultrafast hydrogen-bond dynamics in the infrared spectroscopy of water, *Science* (2003) 301(5640), 1698.
58. Yu. Efimov Effects of the H-bond bridge geometry on the vibrational spectra of water: The simplest models of the H-bond potential, *J. Struct. Chem.* (2008) 49(2) 261-269 [10.1007/s10947-008-0122-4](https://doi.org/10.1007/s10947-008-0122-4)
59. Yu.Ya.Efimov, Yu.I.Naberukhin. Fluctuation theory of hydrogen bonding applied to vibration spectra of HOD molecules in liquid water. II. Infrared spectra: contour shape, integrated intensity, temperature dependence. *Molecular Physics.* (2004)102, 1407-14 .
60. T. Head-Gordon, M. E. Johnson, Tetrahedral structure or chains for liquid water, *Proc. Natl. Acad. Sci. USA* (2006) 103(21), 7973